Title

Mycobacterial Mutagenesis and Drug Resistance Are Controlled by Phosphorylation- and Cardiolipin-Mediated Inhibition of the RecA Coprotease

Journal

Molecular Cell, 72(1)

ISSN

1097-2765

Authors

Wipperman, Matthew F
Heaton, Brook E
Nautiyal, Astha
et al.

Publication Date

2018-10-01

DOI

10.1016/j.molcel.2018.07.037

Peer reviewed

HHS Public Access

Author manuscript

Mol Cell. Author manuscript; available in PMC 2019 October 04.

Published in final edited form as:

Mol Cell. 2018 October 04; 72(1): 152–161.e7. doi:10.1016/j.molcel.2018.07.037.

Mycobacterial Mutagenesis and Drug Resistance Are Controlled by Phosphorylation- and Cardiolipin-Mediated Inhibition of the RecA Coprotease

Matthew F. Wipperman[#1,6], **Brook Heaton**[#7], **Astha Nautiyal**[#1], **Oyindamola Adefisayo**[#3], **Henry Evans**[1], **Richa Gupta**[1], **Dave van Ditmarsch**[1], **Rajesh Soni**[4], **Ron Hendrickson**[4], **Jeff Johnson**[5], **Nevan Krogan**[5], and **Michael S. Glickman**[1,2,3,*]

[1]Immunology Program, Sloan Kettering Institute

[2]Division of Infectious Diseases, Memorial Sloan Kettering Cancer Center

[3]Immunology and Microbial Pathogenesis Graduate Program, Weill Cornell Graduate School.

[4]Microchemistry and Proteomics Core, MSKCC

[5]Department of Cellular and Molecular Pharmacology, UCSF

[6]Clinical and Translational Science Center, Weill Cornell Medicine

[7]Duke University, Department of Molecular Genetics and Microbiology

[#] These authors contributed equally to this work.

Summary

Infection with *Mycobacterium tuberculosis* continues to cause substantial human mortality, in part due to the emergence of antimicrobial resistance. Antimicrobial resistance in Tuberculosis is

[*]Correspondence to the Lead Contact: Michael S. Glickman MD, glickmam@mskcc.org, Immunology Program, Sloan Kettering Institute, 1275 York Ave, New York, NY 10065, 6468882368,.

Author contributions:
Conception (MG, NK, RH)
Supervised experiments (MG, NK, RH, JJ)
Performed experiments: (MW, BH, AN, OA, HE, RG, DvD, RS, JJ)
Specific Figure attribution for shared first authors:
MW: Figures 1D-E, 4A-C, S1, S2A, S3, S5, S7
BH: Figures 1A, 2, 3A-E,G,H, SI Dataset S1
AN: Figures 4D-E, 5B-I, S2B-E,S6
OA: Figures 1B-C, 3A-F, 5A, Dataset S2
Wrote manuscript (MG)
Edited manuscript (MG, MW, AN, OA, NK, BH)

Declaration of Interests

The authors declare no competing interests related to this manuscript.

DATA AND SOFTWARE AVAILABILITY

Software used to perform and plot the evolutionary analyses will be made available on Github at https://github.com/wipperman

In Supplemental Figure S1, for the evolutionary analysis describing the co-occurrence of RecAS207 and NHEJ capability, 128/787 organisms with RecA-N207 were capable of NHEJ, whereas 146/436 organisms with RecA-S207 were capable of NHEJ (Chi-square test: $p << 0.001$).

solely the result of chromosomal mutations that modify drug activators or targets, yet the mechanisms controlling the mycobacterial DNA damage response (DDR) remain incompletely defined. Here we identify RecA serine 207 as a multifunctional signaling hub that controls the DDR in mycobacteria. RecA S207 is phosphorylated after DNA damage, which suppresses the emergence of antibiotic resistance by selectively inhibiting the LexA coprotease function of RecA, without affecting its ATPase or strand exchange functions. Additionally, RecA associates with the cytoplasmic membrane during the mycobacterial DDR, where cardiolipin can specifically inhibit the LexA coprotease function of unmodified, but not S207 phosphorylated, RecA. These findings reveal that RecA S207 controls mutagenesis and antibiotic resistance in mycobacteria through phosphorylation and cardiolipin mediated inhibition of RecA coprotease function.

eTOC

Mutagenic DNA repair is the ultimate cause of antibiotic resistance in *Mycobacterium tuberculosis,* yet the mechanisms that control the genesis of these mutations are incompletely understood. Wipperman et al. identify single residue in the RecA protein that controls mutagenesis in mycobacteria through two parallel mechanisms: phosphorylation and cardiolipin mediated inhibition of the RecA coprotease.

One Sentence Summary:

We identify a single amino acid within Loop2 of RecA that acts a signaling hub for convergent negative feedback of the SOS response

Graphical abstract

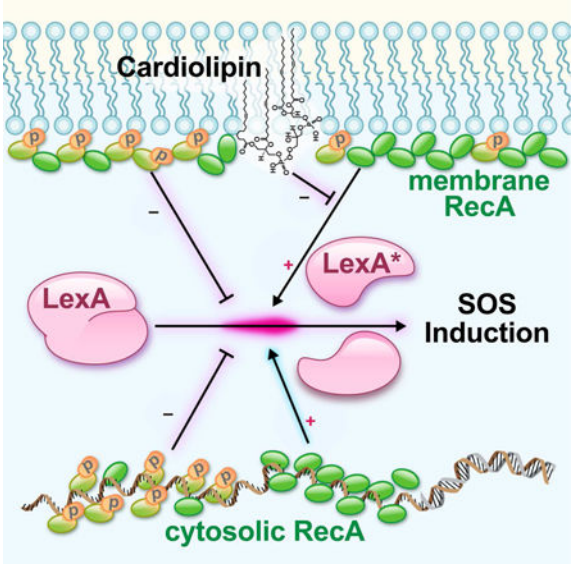

Introduction

Antimicrobial resistance is an escalating global problem that threatens to undermine the efficacy of antibiotics across a wide swath of bacterial infections, including in *M.*

tuberculosis (Mtb), the causative agent of Tuberculosis. In contrast to bacteria that acquire antibiotic resistance through genetic exchange, antibiotic resistance in Mtb is solely the result of chromosomal mutations that inactivate drug targets or drug-activating enzymes. As such, understanding the mechanisms of mutagenesis and DNA repair in mycobacteria is crucial to efforts to control this pathogen. Mycobacteria express a distinctive set of DNA repair pathways, which resemble the eukaryotic suite of double strand break (DSB) repair, including homologous recombination (HR), nonhomologous end joining (NHEJ), and single strand annealing (SSA) (Gong et al., 2004a, 2005, Gupta et al., 2011, 2015). However, despite their centrality to antibiotic resistance, the mechanisms of regulation of the DNA damage response (DDR) and mutagenesis in mycobacteria are incompletely understood.

The classical SOS response controls the DNA damage response in bacteria through transcriptional repression, mediated by the LexA repressor, which undergoes regulated autoproteolysis during the DDR using the scaffold of the RecA nucleoprotein filament as a "coprotease" (Bell and Kowalczykowski, 2016). Mycobacteria utilize a classical SOS response, as well as a LexA independent mechanism (Brooks et al., 2001; Movahedzadeh et al., 1997; Smollett et al., 2012a). However, mutagenesis through the DnaE2 polymerase is LexA controlled and mediates rifampin resistance (Boshoff et al., 2003), indicating that SOS is a major determinant of antibiotic resistance through chromosomal mutagenesis. However, the mechanisms controlling or modifying SOS induction in mycobacteria have not been defined in detail.

Mycobacteria have a suite of eukaryotic like serine-threonine protein kinases (Sherman and Grundner, 2014), which phosphorylate a wide spectrum of proteins in the mycobacterial cell at steady state and in response to stress (Prisic et al., 2010). However, phosphorylation has not been characterized in the context of the mycobacterial DDR. Phosphorylation is a prominent mechanism that controls the eukaryotic DDR (Polo and Jackson, 2011) by modifying protein complex formation or protein function. We postulated that the serine-threonine kinases of mycobacteria could play important roles in the mycobacterial DDR and executed a proteomic screen for phosphorylation events induced by DNA damage. This screen identified a single serine residue within Loop 2 of RecA, which we show is a critical signaling hub for phosphorylation and lipid-based inhibition of SOS induction and mutagenesis in mycobacteria.

Results

A SILAC screen identifies phosphorylation of RecA S207 after DNA damage

We investigated the potential role of phosphorylation in controlling the DDR and mutagenesis in mycobacteria. We designed a SILAC-based proteomic screen (see methods) for phosphopeptides that accumulate after chromosomal double strand DNA breaks (DSB, Figure 1A). The screen utilized conditional expression of the I-SceI homing endonuclease in a doubly lysine/arginine auxotrophic *M. smegmatis* strain that either contains an I-SceI recognition site in the chromosome, or lacks this site. We prepared phosphopeptides one hour after DSB induction and analyzed by quantitative mass spectroscopy in six replicates (3 with each label assignment, see methods). We identified 384 total serine and threonine phosphorylation events, which were spread across diverse protein families (Supplemental

Dataset S1). Phosphorylation on RecA serine 207 was the most strongly induced phosphorylation event in the dataset (Table S1). To confirm the SILAC results, we developed a directed LC-MS/MS assay for the RecA-201–215 peptide. Kinetic quantitation of the RecA peptides after a CRISPR induced DSB revealed that S207 phospho accumulates after a DSB in parallel with the accumulation of RecA, peaking at 7 hours post DSB (Figure 1B-C and Supplemental Dataset S2), confirming the SILAC screen results. Due to variable methionine oxidation of the 201–215 peptide, including synthetic heavy peptides used as standards, we were unable to reliably determine the relative fraction of phosphorylated RecA in the total RecA pool, only the relative increase in phosphorylated RecA compared to control conditions. Nevertheless, these data indicate that RecA S207 phospho accumulates after DNA damage in mycobacteria and prompted us to further dissect the mechanistic effects of this phosphorylation event.

The RecA protein is a central hub of DNA repair transactions in bacteria. A DNA dependent ATPase, RecA polymerizes on single stranded DNA at resected double strand DNA breaks and executes homology search and strand invasion into the homologous DNA duplex (Cox, 2007). The RecA nucleoprotein filament is also a cofactor in transcriptional induction of the DDR through its coprotease activity for the LexA repressor. RecA stimulated autoproteolysis of the LexA repressor derepresses transcription of DNA damage response genes, including the gene encoding the DnaE2 polymerase, which is necessary for mutagenesis in mycobacteria (Boshoff et al., 2003; Smollett et al., 2012a; Warner et al., 2010a). RecA proteins are well conserved across Bacteria, including in the Loop 2 region in which S207 resides. Amino acid sequence alignment of RecA Loop 2 sequences from 1,293 Bacteria and Archaea revealed striking conservation of Loop 2 (L2, Figure 1D), with two residues observed at position 207, a serine or an asparagine, the latter found in *E. coli*. The crystallographic structure of a double stranded DNA-*E. coli* RecA nucleoprotein filament (pdb: 3CMX) revealed L2 to be intimately associated with DNA where it delineates the trinucleotide triplet associated with each RecA protomer (Chen et al., 2008). Phosphorylation within loop 2 could therefore affect DNA binding, filament structure, or strand exchange (Figure 1E). We analyzed the co-occurrence of serine at position 207 in L2 with the gene encoding the Ku protein, absent in *E. coli* and a central mediator of NHEJ in Bacteria (Gong et al., 2004b, 2005; Gupta et al., 2011), and found a highly significant association between the presence of a serine residue and an NHEJ pathway (Figure S1).

RecA L2 phosphorylation inhibits DNA repair

To examine the function of L2 phosphorylation in the mycobacterial DDR, we deleted *recA* from *Mycobacterium smegmatis* and *Mycobacterium tuberculosis* and complemented these null strains with RecA alleles encoding amino acid substitutions that either ablate phosphorylation (S207A) or mimic phosphorylation (S207D or S207E). All RecA proteins accumulated to similar levels (Figure 2A), indicating that the amino acid substitutions do not impair protein stability. Mycobacterial cells lacking RecA are highly sensitive to DNA damage, as previously reported (Gupta et al., 2011). Phosphoablative substitution at S207 had no effect on DNA damage sensitivity in *M. smegmatis* to either UV light or ionizing radiation (IR) (Fig 2B,D), or in *M. tuberculosis* to UV (Figure 2E) or methyl methanesulfonate (Fig 2F), demonstrating that serine 207, or its phosphorylation, are not

required for RecA function in repair. In contrast, the phosphomimetic substitutions (S207E or S207D) of S207 sensitized *M. smegmatis* to UV (Figure 2B,C) and ionizing radiation (IR) (Figure 2D). *M. tuberculosis* expressing RecA S207E was as sensitive to UV (Figure 2E) or MMS (Figure 2F) as cells lacking RecA altogether. These data indicate that phosphorylation of RecA S207 inhibits RecA function during mycobacterial DNA repair.

RecA phosphorylation inhibits the SOS response

RecA has multiple functions in the DNA damage response, including directly mediating homology search for DSB repair and inducing SOS through its LexA coprotease function. To examine whether RecAS207 phosphorylation affects SOS induction, we quantitated the SOS response by measuring induction of *dnaE2,* a LexA-repressed gene required for mutagenesis in mycobacteria (Boshoff et al., 2003; Warner et al., 2010b). We observed robust induction of *dnaE2* transcription after quinolone-induced DSBs or UV light in *M. smegmatis* (Figure 3A,B) or *M. tuberculosis* (Figure 3C). Phosphomimetic substitution at S207 (either S207D or S207E) strongly inhibited *dnaE2* induction in both *M. smegmatis* (Fig 3A,B) and *M. tuberculosis* (Fig 3C), whereas the phosphoablative mutation caused hyperinduction of *dnaE2* (Fig 3A). To better understand the effect of RecA L2 phosphorylation on the kinetics of SOS resolution, we exposed *M. smegmatis* to a transient DSB using quinolone antibiotics and followed the *dnaE2* mRNA for 6 hours post exposure. Peak SOS was observed at the end of the clastogen exposure, with phosphomimetic substitution suppressing SOS induction, as reported above. However, at a time when cells with wild type RecA began to resolve SOS induction, phosphoablative substitution in L2 caused persistence of SOS induction, indicating that phosphorylation serves to shut off the SOS response once DNA damage is removed (Fig 3D).

To determine if the inhibition of SOS by RecA S207 phosphorylation was accompanied by suppression of chromosomal mutagenesis, we assayed Rifampin (Rif) resistance, caused by mutations in the β-subunit of RNA polymerase, and previously shown to be dependent on *dnaE2* (Boshoff et al., 2003; Warner et al., 2010b). *M. smegmatis* or *M. tuberculosis* Δ*recA* cells were unable to evolve Rif resistance, consistent with an inability to induce SOS (Figure 3E, F). We observed strong inhibition of mutagenesis in the *M. smegmatis* and *M. tuberculosis* phosphomimetic strains (Figure 3E,F), and hypermutagenesis in the *M. smegmatis* phosphoablative strain (Figure 3E). These data indicate that phosphorylation of RecA strongly inhibits the transcriptional induction and downstream mutagenesis controlled by the SOS response.

To ask whether phosphorylation dependent suppression of SOS accounts for clastogen sensitivity of mycobacteria with constitutively phosphorylated S207, we overexpressed the LexA repressor, reasoning that an increased cellular concentration of LexA might reveal differences in the efficiency of LexA cleavage in RecA phosphomimetic and ablative mutants. Overexpression of LexA mildly but significantly sensitized wild type cells to UV damage, but had no effect on cells lacking RecA, as predicted (Fig 3G). RecAS207A cells were resistant to the sensitizing effect of LexA overexpression, consistent with a hypermorphic coprotease activity (Fig 3G). In contrast, RecAS207E cells were highly sensitized by LexA overexpression, by a factor of 100X from an already sensitized baseline

(Fig 3G). To further confirm these findings, we expressed a LexA protein with a mutation that prevents autoproteolysis (S167A) and therefore cannot be activated by RecA. Expression of LexA S167A sensitized wild type cells to ionizing radiation, consistent with an inhibited SOS response (Fig 3H). RecAS207A cells were resistant to the effects of uncleavable LexA, again consistent with a hypermorphic LexA cleavage phenotype. In contrast, cells with RecA S207E were not further sensitized by LexAS167A (Fig 3H), consistent with an already inhibited SOS response that cannot be further dampened. Taken together, these data indicate that phosphorylation of RecA at S207 controls the RecA LexA coprotease function in vivo

RecA phosphorylation controls the LexA coprotease activity of RecA

The strong inhibition of SOS response and mutagenesis observed with phosphomimetic substitution at S207 could reflect several defects in RecA protein function. The scaffold for LexA autoproteolysis is the RecA nucleoprotein filament, and therefore biochemical defects in RecA DNA binding, ATPase, or polymerization on ssDNA could lead to failure to activate SOS. We proceeded to interrogate the biochemical properties of RecA proteins substituted at S207. We purified RecA, RecAS207A, RecAS207E, and RecAS207D to homogeneity (Fig S2A) and tested these proteins for DNA stimulated ATPase, DNA binding, and strand exchange activity. We observed that substitution at S207 had no demonstrable effect on ATPase activity (Figs 4A, S2B-E). However, there was a noticeable impairment of DNA binding for the phosphomimetic RecA mutants, S207E and S207D (Figure 4B).

We next tested the ability of RecA proteins to catalyze transfer of a fluorescently labeled oligonucleotide to homologous ϕX174 RF1 plasmid DNA to form a D loop. Strand transfer was dependent on RecA, nucleotide, and magnesium (Fig S3A). Mycobacterial RecA is significantly less active than *E. coli* RecA, but nevertheless was active in D loop formation (Fig 4C, S3B). Despite the impaired DNA binding observed, we observed that phosphomimetic or phosphoablative substitutions at S207 did not demonstrably affect RecA strand exchange activity (Fig 4C, S3B), indicating that the in vivo damage sensitivity of this mutant is unlikely to reflect defective homologous recombination. These data indicate that phosphorylation of S207 does not impair the DNA stimulated ATPase or strand exchange activities of RecA.

We next asked whether modification of residue 207 affects cleavage of the LexA repressor. We reconstituted the LexA cleavage reaction in vitro using RecA nucleoprotein filaments (Nautiyal et al., 2014) and purified mycobacterial LexA protein (Fig S2A). RecA filaments catalyzed cleavage of the LexA protein over the course of a 25 minute reaction (Fig 4D,E). However, phosphomimetic substitutions at S207 impaired the LexA coprotease function of RecA (Figure 4D, E), with S207E showing severely impaired coprotease function. We also observed a mild impairment of coprotease function for S207A, indicating that the serine is also important for coprotease function independent of phosphorylation. These data indicate that L2 phosphorylation selectively impairs the coprotease function of RecA, while preserving other repair functions of this multifunctional protein.

RecA associates with the cytoplasmic membrane during the DDR

Recent data (Lesterlin et al., 2013; Rajendram et al., 2015; Zhang et al., 2016) in *E. coli* has rejuvenated interest in the older finding that *E. coli* RecA associates with the cytoplasmic membrane after DNA damage (Garvey et al., 1985). *E. coli* RecA associates with anionic phospholipids through the L2 region (Rajendram et al., 2015; Zhang et al., 2016), the site of phosphorylation in mycobacterial RecA. Proteomic studies of mycobacterial membranes have identified RecA as membrane associated, specifically in the plasma membrane-cell wall fractions, although these studies were not performed after DNA damage (Hayashi et al., 2016a). These studies suggest that L2, in addition to its role in phosphorylation dependent regulation of SOS, could have a second role in mediating membrane interactions of RecA. We first examined the in vivo dynamics of RecA GFP fusions with substitutions at S207. After confirming that these fusions accumulated after DNA damage (Fig S4A) and complemented the clastogen sensitivity defect of Δ*recA* (Fig S4B,C), we imaged RecA filament formation by fluorescence microscopy. DNA damage caused obvious accumulation of large RecA bundles that in many cases spanned the cell length, as has been observed in *E. coli* (Lesterlin et al., 2013), but GFP fusions to RecA carrying phosphoablative and phosphomimetic mutations at S207 were indistinguishable from WT (Fig S4D).

To more sensitively determine whether RecA associates with membranes, we adopted a biochemical approach. We fractionated *M. smegmatis* cell lysates before and after DNA damage to separate cytosolic and membrane fractions (Hayashi et al., 2016b). Western blotting with antibodies to the membrane protein FtsY and cytosolic protein RpoB identified membrane and cytosolic fractions, respectively (Fig 5A). Probing of cellular fractions with anti-RecA antibodies clearly revealed RecA to be cytosolic in unstressed cells (Fig 5A). After DNA damage, a fraction of cellular RecA associates with the membrane (Fig. 5A), consistent with findings in *E. coli.* We did not observe any alteration in the proportion of the RecA-S207A or S207E proteins associated with the membrane during DNA damage, indicating that S207, or its phosphorylation, does not control membrane localization.

Cardiolipin specifically impairs the LexA coprotease activity of mycobacterial RecA

The association of RecA with the membrane may suggest that membrane localization of RecA modulates RecA activity during the DDR. The mycobacterial inner membrane is composed of a mixture of mannosylated glycolipids, phospholipids, and cardiolipin (Bansal-Mutalik and Nikaido, 2014). Phospholipids were recently implicated in RecA function in *E. coli* through inhibition of the RecA ATPase (Rajendram et al., 2015; Zhang et al., 2016). We hypothesized that these lipids might modify RecA function in mycobacteria. To test this idea, we generated 100 μm unilamellar liposomes containing different ratios of anionic phospholipids (Fig S5A) and tested their effects on RecA biochemical activities in vitro. We observed no effect of phospholipid-containing liposomes on RecA ATPase (Fig S5B-D), DNA binding (Fig S6A), or strand exchange activities (Fig S6B) indicating that phospholipids do not inhibit ATP hydrolysis, DNA binding, or nucleoprotein filament formation. However, although phosphatidylglycerol liposomes had no effect on LexA coprotease activity (Fig 5B, C), we observed a strong dose dependent inhibition of RecA LexA coprotease activity by cardiolipin-containing vesicles. Vesicles containing 80:20 DOPG:cardiolipin completely abolished coprotease activity (Figure 5B,C). However, the

inhibitory effect of cardiolipin is dependent on serine 207 in loop 2. The already inhibited LexA coprotease of the RecAS207E protein was not further inhibited by cardiolipin (Fig 5D) and the S207A coprotease activity was also less sensitive to lipid inhibition (Fig. 5E). These data demonstrate a specific effect of cardiolipin in inhibiting RecA coprotease function through the S207 residue in Loop 2, and that posttranslational modification of this residue confers resistance to lipid inhibition.

Recent studies in *E. coli* (Rajendram et al., 2015) implicated cardiolipin in promoting the SOS response in vivo, hypothesized to be through stabilization of RecA filaments through cardiolipin inhibited ATPase activity. Because this effect contrasts with the inhibition of mycobacterial LexA cleavage we observe, we examined the effect of an asparagine substitution at S207 to mimic the *E. coli* L2 residue. Nucleoprotein filaments formed from RecA S207N were competent as a coprotease but were resistant to the inhibitory effect of cardiolipin (Figure 5F). We also reconstituted the LexA cleavage reaction using *E. coli* RecA and LexA and tested the effect of cardiolipin. We observed that *E. coli* RecA catalyzed LexA cleavage is faster than the mycobacterial reaction over an 8-minute time course (Fig 5G). In contrast to the inhibition of LexA cleavage by cardiolipin observed with mycobacterial proteins, phosophlipids actually accelerated the *E. coli* reaction, consistent with previous reports (Fig 5G,H). These data indicate that cardiolipin inhibits the mycobacterial DDR through phospholipid inhibition of RecA coprotease activity, an effect that is controlled by the phosphorylation status of serine 207 in RecA L2.

Discussion

We have identified a single serine in RecA L2 as a critical signaling hub for the mycobacterial DNA damage response. We find that RecA phosphorylation on Serine 207 attenuates the SOS response, and the downstream mutagenesis mediated by SOS, through its specific inhibitory effect on LexA coprotease function, despite preservation of other RecA functions in DSB repair (Figure 6). This phosphorylation-dependent inhibition of LexA cleavage implicates post-translational modification of L2 in the coprotease activity of RecA nucleoprotein filaments. Although detailed studies have not been performed on the critical residues in mycobacterial RecA required for LexA cleavage, prior saturation mutagenesis studies of *E. coli* L2 found that alanine substitution at N206 (the equivalent residue to S207 in mycobacteria) impaired both recombination and clastogen resistance function of RecA in vivo, suggesting substantial differences in the function of *E. coli* and mycobacterial RecA. One explanation for the inhibition of LexA proteolysis by phosphorylation is that the posttranslational modification of S207 impairs the direct interaction of the LexA repressor with the RecA filament. Alternatively, modification of S207 could recruit an inhibitory factor that occludes the LexA interaction site on RecA.

The second mechanism by which RecA serine 207 attenuates the SOS response is through lipid inhibition of the RecA protein. We find that RecA is sequestered at the membrane during the DDR, a compartmentalization that brings RecA in contact with cardiolipin, a major component of the mycobacterial inner membrane (Hayashi et al., 2016b; Morita et al., 2006), which strongly and specifically inhibits the LexA coprotease activity of RecA without affecting other repair functions. Although S207, or its phosphorylation, are not

required for membrane association, this residue is critical for cardiolipin based inhibition. Phosphorylated RecA is resistant to further inhibition by cardiolipin, indicating that these mechanisms operate in parallel to control RecA function. In *E. coli,* recent data indicates that Loop 2 of RecA specifically binds phospholipids, including cardiolipin (Rajendram et al., 2015; Zhang et al., 2016). The biochemical effect of phospholipids on *E. coli* RecA is ATPase inhibition in vitro, which stabilizes RecA filaments in vivo. Thus, in *E. coli,* phospholipids support a robust SOS response through stabilization of the RecA filament and its LexA coprotease activity. Our findings confirm a critical role for the membrane and cardiolipin in regulating RecA function, but indicate that the specific mechanisms of this effect in mycobacteria differ substantially from *E. coli*. In mycobacteria, cardiolipin strongly inhibits RecA catalyzed LexA cleavage, without affecting ATPase activity or strand exchange. Thus, in mycobacteria, phospholipids and the membrane suppress SOS and mutagenesis.

The existence of phosphorylation and lipid-based mechanisms that dampen the SOS response indicates that the mycobacterial cell employs counterregulatory mechanisms to avoid unopposed SOS induction. The LexA gene in mycobacteria is autoregulated (Davis et al., 2002; Smollett et al., 2012b), indicating that SOS induction leads to synthesis of additional LexA protein, which, in the setting of persistent RecA filaments to act as coprotease, will continually amplify the SOS response in a positive feedback loop. As coprotease-competent RecA filaments persist in the cell, a mechanism is needed to dampen the SOS response, while preserving the other repair functions of RecA, which may still be required to repair the initiating damage. Our data supports that L2 is a critical signaling hub for this negative feedback loop through two mechanisms (Figure 6). Our data supports a model in which there are two pools of RecA during the DDR—cytoplasmic and membrane bound. The cytoplasmic RecA pool can be inhibited by phosphorylation on S207, whereas non-phosphorylated RecA is competent for SOS induction. The membrane bound RecA pool is subject to both phosphorylation and cardiolipin based inhibition, but these mechanisms are parallel rather than additive as the unmodified S207 residue is required for cardiolipin inhibition.

Our findings have important implications for understanding mutagenesis and antibiotic resistance in mycobacteria. The finding that phosphorylation of RecA dramatically suppresses its promutagenic role implies that dynamic changes in kinase signaling induced by the environment or membrane damage could modify the mutagenic state of *M. tuberculosis,* thereby promoting antibiotic resistance mutations under stress. In addition, these findings implicate phosphorylation as an important mediator of the DDR in mycobacteria, further extending the already extensive similarities between mycobacterial and eukaryotic DNA repair. Our identification of this mechanism controlling prokaryotic DNA repair provides a novel point of intervention to counteract antibiotic resistance through chromosomal mutagenesis in mycobacteria, including *Mycobacterium tuberculosis.*

STAR+METHODS

EXPERIMENTAL MODELS AND SUBJECT DETAILS

Bacterial strains

Mycobacterium smegmatis strains were derivatives of *mc*^{2}*155.* Gene deletions were made by homologous recombination and double negative selection. *Mycobacterium tuberculosis* strains are on the Erdman EG2 background, an animal passaged, PDIM$^+$ strain.

METHOD DETAILS

SILAC

Cultures were grown to saturation in 7H9+ADS, Hygromycin, Kanamycin, 40 μg/mL Lysine, 240 μM Arginine. Cultures were then diluted to 0.02 in 7H9+ADS, Hygromycin, Kanamycin, and 40 μ,g/mL Lysine, 240 μM Arginine, or the same concentration of ^{13}C Lysine, ^{13}C Arginine. At OD_{600} = 0.5 100 ng/mL ATc was added for 1 hour to induce I-SceI expression. Cells were collected at 3,700×g for 10 minutes at 4 °C and resuspended in 8 M Urea, 0.1 M Tris-HCl (pH = 7.9), 150 mM NaCl, 200ul of both phosphatase inhibitors cocktails 2 and 3 and protease inhibitor (0.4ml of 25× cOmplete™ Protease Inhibitor Cocktail). Cells were lysed using sonication 3 times for 1 minute at 30%. Lysates were then clarified at 4 °C for 10 minutes at 20,000×g.

Sample preparation for SILAC Mass spectrometry analysis

Disulfide bonds were reduced by incubation with 4 mM TCEP for 30 minutes at room temperature, and free sulfhydryl groups were alkylated by incubation with 20 mM iodoacetamide for 30 minutes at room temperature in the dark. Samples were diluted back to 2 M urea by addition of 0.1 M Tris-HCl (pH = 8.0), and trypsin was added at an enzyme:substrate ratio of 1:100. Lysates were digested overnight at 37 °C. Following digestion, the samples were concentrated using SepPak C18 cartridges. The C18 cartridge was washed once with 1 mL of 80% acetonitrile, 0.1% trifluoroacetic acid, followed by a 3 mL wash with 0.1% TFA. 10% TFA was added to each sample to a final concentration of 0.1% after which the samples bound to the cartridge. The cartridge was washed with 3 mL of 0.1% TFA after binding, and the peptides were eluted with 40% ACN, 0.1% TFA. Following elution, the peptides were lyophilized to remove all water and organic solvent.

Phosphopeptides were fractionated using hydrophilic interaction chromatography (HILIC). Buffers used for HILIC separation were HILIC buffer A (2% ACN, 0.1% TFA) and HILIC buffer B (98% ACN, 0.1% TFA). Peptides were resuspended in 90% HILIC buffer B and loaded onto a TSKgel amide-80 column. Peptides were separated at a flow rate of 0.5 mL/min using a gradient from 90% to 85% HILIC buffer B for 5 minutes, 85% to 55% HILIC buffer B for 80 minutes, then 55% to 0% HILIC buffer B for 5 minutes. Fractions were collected every 2 minutes and the 22 fractions previously determined to contain the majority of phosphopeptides were lyophilized. Following HILIC fractionation, fractions were further enriched for phosphopeptides using titanium dioxide magnetic beads using the

manufacturer's protocol. Following titanium dioxide enrichment, sample were lyophilized and resuspended in 0.1% formic acid for mass spectrometry analysis.

Mass spectrometry analysis of RecA phosphosite

Cells were collected and washed twice with ice cold phosphate-buffered saline (155 mM NaCl, 3 mM Na_2HPO_4, 1 mM KH_2PO_4, pH = 7.4, PBS) and frozen in liquid N_2. For lysis, bacterial cells were thawed on ice and lysed in lysis buffer (8 M urea, 25 mM Tris-HCl, 150 mM NaCl, phosphatase inhibitor 2 and 3 and protease inhibitors. Lysates were sonicated three times at 30 – 40% power for 15 s each with intermittent cooling on ice, followed by centrifugation at 14,000 rpm for 30 min at 4 °C. The supernatants were transferred to a new tube and the protein concentration was determined using a BCA assay. For each time point, 5 mg of total protein was used. Protein was reduced with 5 mM DTT at 56 °C for 30 min, cooled to room temperature, and alkylated with 11 mM iodoacetamide in the dark at room temperature for 30 min. The alkylation was then quenched by the addition of an additional 5 mM DTT. Samples were diluted 6-fold with 50 mM NH_4HCO_3 and digested overnight with trypsin (1:50) at 37 °C. The next day, the digestion was stopped by the addition of 0.25% TFA (final v/v) and centrifuged at 10,000 rpm for 10 min at room temperature to pellet precipitated lipids and collected the cleared supernatant. Supernatant were desalted on a SepPak C18 cartridge 500 mg. Desalted sample (1%) was directly injected to LC-MS/MS to quantify unmodified RecA peptides and remaining 99% of sample was lyophilized for phosphopeptides enrichment.

RecA phosphopeptides enrichment

Phosphopeptide enrichment was performed as described (Adachi et al., 2016), with minor modifications. 5 mg of lyophilized peptides were resuspended in 500 μL of binding buffer (2 M lactic acid in 50% ACN). Resuspended peptides were incubated with 20 mg of titanium dioxide microspheres for one hour, by a thermostat vortex mixer on the highest speed setting at room temperature. Afterwards, the beads were washed twice with 500 μL of the binding solution and three times with 500 μL (50% ACN / 0.1% TFA), and phosphopeptides were eluted sequentially with 60 μL of 5% ammonium hydroxide, 5% piperdine and 5% pyrrolidine solution. Peptide elutions were combined and quenched with 120 μL of 50% ACN / 5% formic acid and were dried by speedvac. Enriched phosphopeptides were further fractionated in seven fractions with stepwise elution by TFA and ammonium acetate using SDB-SCX Stage-Tip (Kettenbach and Gerber, 2011). The elution buffer contained 0.5% TFA, 30% ACN for fraction 1; 1% TFA, 30% ACN for fraction 2; 2% TFA, 30% ACN for fraction 3; 3% TFA, 30% ACN for fraction 4; 3% TFA, 30% ACN, 100 mM ammonium acetate for fraction 5; 3% TFA, 30% ACN, 500 mM ammonium acetate for fraction 6; 30% ACN, 100 mM ammonium acetate for fraction 7.

LC-MS/MS analysis:

Desalted peptides and fractionated phosphopeptides were resuspended in 10 μL of 3% ACN/ 0.1% formic acid and were injected onto a C18 capillary column on a nano ACQUITY UPLC system (Water) which was coupled to the Q Exactive plus mass spectrometer. Peptides were eluted with a non-linear 110 min gradient of 0.5 – 50% buffer B (0.1% (v/v) formic acid, 100% ACN) at a flow rate of 300 nL/min. After each gradient, the column was

washed with 90% buffer B for 5 min and re-equilibrated with 99.5% buffer A (0.1% formic acid, 100% HPLC-grade water).

MS data were acquired with combined two scan events corresponding full scan and a Parallel Reaction Monitoring (PRM) method targeting the eight RecA peptides. Target value for the full scan MS spectra was 1×10^6 ions in the 380–2000 *m/z* range with a maximum injection time of 30 ms and resolution of 70,000 at 200 *m/z* with data collected in profile mode. The PRM method employed at resolution of 17,000 at 200 *m/z,* a target AGC value 2×10^5 and maximum fill times of 100 ms. The precursors ions of each targeted peptide were isolated using a 1.5 *m/z* unit window and fragmented by higher-energy C-trap dissociation with normalized collision energy of 27 eV.

Data processing:

Data analysis was performed using Xcalibur (version: 4.0.27.19, Thermo Fisher Scientific) and the area under the curve of selected intense fragment ions summed to determine the quantity of the respective peptide.

DNA Damage assays

M. smegmatis strains were grown in LB with 0.5% glycerol, 0.05% tween80, 0.5% dextrose, 20 μg/ml streptomycin until they reached saturation. *M. tuberculosis* strains were grown in 7H9 medium + OADC + 20 μg/mL Kanamycin to saturation. Cultures were diluted to an OD_{600} = 0.02 *(M. smegmatis)* or 0.1 *(M. tuberculosis)* and grown to OD_{600} = 0.6, washed once with an PBS + 0.05% tween80 and serially diluted onto 7H10 agar plates. Agar plates were treated with various doses of UV radiation with a Stratagene UV stratalinker 1800. Plates were wrapped in foil (to prevent potential effects of photolyase) and incubated at 37°C. For treatment with the clastogen methyl methanesulfonate (MMS), *M. tuberculosis* was grown as indicated above to an OD_{600} of 0.5 and treated with PBS or 0.2% MMS (final) for 1 hour. Cultures were washed with PBS + 0.05% tween80 three times to remove MMS and then diluted to an OD_{600} = 0.03. Growth was measured by OD_{600} for 10 days. For ionizing radiation exposure, cells were grown to saturation in 10 mL of LB media and then diluted in fresh media. When cultures reached OD_{600} ~ 0.3, they were centrifuged and resuspended in 5 mL of PBS with 0.05% tween80. 100 μL aliquots were treated with IR from a ^{137}Cs source that delivers 10 Gray/min on a rotating platform to ensure uniform exposure. Pooled aliquots were used for plating dilutions. Ciprofloxacin exposure was at 10 μg/mL for 1 or 3 hours.

Western Blot

Lysates were prepared from cells at OD600 of 0.6 and protein quantities were roughly normalized to equivalent cell number. Equal loading was confirmed with RpoB antibodies as a loading control. Commercially available anti-RecA (Abcam 63797) was used at a 1:3,000 dilution and anti-RpoB was used at a 1:20,000 dilution, both incubated for 1 hour. Anti-RecA antisera were raised in rabbits against purified full-length *M. smegmatis* RecA.

RecA and LexA protein purification

The following buffers were used: **buffer A** (binding): 20 mM Tris-HCl (pH = 8.0), 200 mM NaCl, 50 mM imidazole, 10% glycerol; **buffer B** (wash): 20 mM Tris-HCl (pH = 8.0), 2 M KCl; **buffer C** (elution): 20 mM Tris-HCl (pH = 8.0), 0.2 M NaCl, 0.5 M imidazole, 10% glycerol; **buffer D** (dialysis): 20 mM Tris-HCl (pH = 8.0), 0.2 M NaCl, 10% glycerol; **buffer E** (lipid vesicle buffer): 20 mM Tris-HCl (pH = 8.0). *M. smegmatis recA* WT, S207A, S207E S207D and LexA were cloned into the pET-Sumo protein expression vector, containing a N-terminal polyhistidine (His_6) tag, SUMO, and a Ulp1 cleavage site. DNA sequencing confirmed the full gene was present in each instance without mutations. T7-based expression in ER2566 or BL21-CodonPlus (DE3) expression strain of *E. coli.* was induced with 0.3 mM isopropyl-β-d-thiogalactoside (IPTG) for 4 hours at 37 °C. Cells were collected by centrifugation and resuspended in buffer A and lysed by sonication. Lysate was centrifuged at 20,000 × g at 4 °C for 30 minutes. Supernatant was passed over a Ni-NTA or Talon column for immobilized metal affinity chromatography purification, washed with 10 column volumes of buffer A, then buffer B to remove DNA. Protein was eluted with buffer C. Eluted protein was dialyzed overnight in buffer D with ~0.3 mg of His_6-labeled Ulp1 protease, which was expressed recombinantly in *E. coli* and purified. After cleavage protein was run over Ni-NTA column and the flow through was collected containing purified RecA or LexA protein. Isolated proteins in buffer D were concentrated by ultrafiltration (molecular weight cutoff: 10 kDa) to less than 0.5 mL and directly frozen. Purified RecA WT, S207A, S207E, S207D, and S207N proteins were analyzed by reducing SDS-PAGE, and protein band identities and mutant L2 amino acid substitutions were confirmed by in-gel tryptic digestion and subsequent LC-MS/MS analysis.

Strand exchange assay

A reaction mixture containing Tris-HCl (70 mM, pH = 7.6), $MgCl_2$ (10 mM), dithiothreitol (5 mM), ATPγS (2.0 mM), RecA (5.0 μM), 100 nM HPLC-purified 5’ NHS ester Alexa Fluor 488-labeled oligo (IDT), with the following sequence: /5Alex488N/GA AAA TTC GAC CTA TCC TTG CGC AGC TCG AGA AGC TCT TAC TTT GCG ACC TTT CGC CAT C (referred to as 488N-ϕX174-oligo), was incubated at 37 °C for 10 minutes to form RecA-ssDNA filaments. D loop formation was initiated with the addition of 1 μg ϕX174 RF1 DNA to the mixture, and incubated at 37 °C. The reaction was stopped via addition of Proteinase K and 1% SDS at room temperature. Reaction products were resolved on a 1% agarose gel and imaged on a Typhoon Trio Variable Mode Imager in the green channel (PMT 600, laser 532 nm, normal sensitivity, 100 μm^2 pixel size).

ATPase assay

The ATPase assay was performed in a 10 μL reaction volume containing 70 mM Tris-HCl (pH 7.6), 5 mM DTT, 10 mM $MgCl_2$, and 10 μM ϕX174-oligo + 3 μM RecA. The reaction was initiated by the addition of 2 mM [$\gamma-^{32}P$] ATP and incubated for different time intervals (0,10,20,30,40,50,60 min) at 37 °C. The reaction was stopped by the addition of 25 mM EDTA. Aliquots (2 μL) were transferred onto polyethylenimine cellulose F sheets and developed with a solution containing 0.5 M LiCl and 1 M formic acid. The TLC sheets were air dried and the bands were visualized using a Typhoon Trio Variable Mode Imager. The

band intensities were quantified using Image J and plotted using GraphPad prism (version 7.0). To monitor the effect of lipid vesicles, the reaction mixtures was incubated either in the presence of 100% DOPG vesicles or DOPG:CL vesicles. The reaction was initiated by the addition of 2 mM [$\gamma-^{32}$P] ATP and incubated for 30 minutes. The reaction products were resolved by thin layer chromatography (TLC) on polyethylenimine (PEI) cellulose F plates (Merck Millipore).

LexA cleavage assay

The LexA cleavage assay was performed in a 10 μL reaction volume containing Tris-HCl (70 mM, pH = 7.6), $MgCl_2$ (10 mM), dithiothreitol (5 mM), ATPγS (3 mM), RecA (3 μM), 10 μM ssDNA with the following sequence GAT GGC GAA AGG TCG CAA AGT AAG AGC TTC TCG AGC TGC GCA AGG ATA GGT CGA ATT TTC. The reaction mixtures were incubated at 37 °C for 15 min. Subsequently, 10 μM LexA was added and further incubated for different time intervals (0, 5, 10, 15, 20 and 25 min) at 37 °C. Samples were separated by SDS-PAGE followed by staining with Coomassie Blue. The band intensities were quantified using Image J and plotted using GraphPad prism (version 7.0). To monitor the effect of lipid vesicles, the reaction was incubated in the presence of 100% DOPG or DOPG:CL vesicles, Tris-HCl (70 mM, pH = 7.6), $MgCl_2$ (10 mM), dithiothreitol (5 mM), ATPγS (3 mM), RecA (3 μM), 10 μM oligodT_{30} ssDNA. The reaction was incubated at 37 °C for 15 minutes and 5 μM LexA was added and further incubated for different time intervals (0, 5, 10, 15, 20 and 25 min) at 37 °C. The reaction was terminated by boiling in SDS sample buffer. Samples were separated by SDS-PAGE followed by staining with Coomassie Blue. The band intensities were quantified using Image J and plotted using GraphPad prism (version 7.0).

Electrophoretic mobility shift (EMSA) assay

Reactions contained Tris-HCI (70 mM, pH = 7.6), $MgCl_2$ (10 mM), dithiothreitol (5 mM), ATPγS (2.0 mM), RecA (variable concentrations), and 488N-ϕX174-oligo chemically labeled with Alexa Fluor 488 (250 nM) were combined to a final volume of 10 μL and incubated at 37 °C for 30 minutes to form RecA-ssDNA filaments. The reaction products were resolved on a 1% agarose gel and imaged on a Typhoon Trio Variable Mode Imager in the green channel (vide supra).

UV induced mutagenesis

10 mL of each strain at OD_{600} = 0.6 was transferred to Omnitray single-well plates and exposed to 20 mJ/cm^2 UV radiation using a Stratagene UV stratalinker 1800. From each treated sample and its untreated control, 5 mL of culture was transferred to 5 mL of fresh media and shaken at 37 °C /150 RPM for 3 hours. From each sample, 1 mL of culture was cultured in duplicate on 7H10 agar plates containing 0.5% glycerol, 0.5% dextrose, and 40 μg/mL rifampicin and incubated at 37 °C for 72 hours to determine rifampicin-resistant CFU. Additional duplicates were taken from each sample and dilution-plated on 7H10 agar containing no antibiotic to determine viable CFU. Resistant mutants were then normalized to viable CFU for each set of samples, 10 replicates for each strain. Graph represents average rifampicin-resistant mutants per viable CFU. Error bars represent 95% confidence intervals.

Lipid vesicle preparation

100-nm diameter unilamellar vesicles (large unilamellar vesicles) were made from mixtures of lipids by extrusion. Lipid ratios were determined by mass. The lipids dissolved in organic solvent were mixed proportionally according to their mass, dried as a thin film under N_2, and evacuated via lyophilizing overnight. The lipid mixtures were re-suspended in buffer E, sonicated, and vortexed. Each sample underwent at least two freeze-thaw cycles at –80 °C and 37 °C. This mixture was extruded with an Avanti Mini-Extruder Set at least 10 times through two stacked 100-nm filters, yielding homogeneous batches of unilamellar vesicles. The size of the vesicles was confirmed by dynamic light scattering, and net charge (Zeta potential) was measured.

RT-qPCR

Cultures with 1.25 μg/ml Ciprofloxacin were shaken at 37 °C /150RPM for 3 hours. 10 mL samples were collected from each culture in duplicate for RNA preparation. 500 ng of RNA was used to make cDNA using the Thermo Maxima First Strand cDNA synthesis kit for RT-qPCR with dsDNase. RT-qPCR was performed using TaqMan Assay with SigA as the housekeeping gene and comparing the ΔΔCT for each strain treated for 3 hours to its respective untreated control.

M. tuberculosis strains were grown in 7H9 medium+OADC to OD_{600} = 0.6 at 37 °C. For each strain, 8 mL of culture was transferred to Extra-Depth disposable petri dish and exposed to ~20mJ/cm^2 UV radiation using a Stratagene UV stratalinker. From each treated sample and untreated controls 5 mL of culture were transferred to a 30 mL bottle containing 5 mL of fresh media and shaken at 37 °C/150 RPM for ~24 hours. 5 mL samples of untreated culture from each strain were also transferred to 5 mL of fresh media and shaken at 37 °C/150 RPM for ~24 hours. Cell pellets were lysed in TRIzol reagent by bead beating 3 times for 45 s and processed using the Direct-zol Miniprep Plus kit. RNA was treated following the rigorous DNase treatment of the TURBO DNA-free kit. cDNA synthesis and RT-qPCR were similar to protocol used for *M. smegmatis* cells. Primers for RT-qPCR:

M.smegmatis dnaE2 forward primer: GCACTGGCACATCCTCAC

M.smegmatis dnaE2 reverse primer: CCGAACCGGTCCACTAGAT

M.smegmatis dnaE2 TaqMan probe: ACATGGCCTTTGCGGCATCC

M. tuberculosis dnaE2 forward primer: GTCCTGCAATGGGACAAAGA

M. tuberculosis dnaE2 reverse primer: CACCAGGTCTTTCGCATAGT

M. tuberculosis dnaE2 TaqMan probe: CGGCAATCGGCTTGGTGAAATTCG

Cell fractionation

The indicated strains were exposed to ciprofloxacin as detailed under RT-qPCR. Cells were washed twice with 50 mM HEPES (pH = 7.4) and snap frozen on dry ice, resuspended to 20 mL of 50 mM HEPES (pH = 7.4), and lysed three times via French press at 14,000 psi.

9.5ml of the lysates were spin concentrated at 3,7 00G for 15mins two times in an Amicon Ultra −15 Centrifugal unit (Ultracel −10K) and then 600ul of the concentrated lysate was overlaid on a continuous sucrose gradient of 20 – 60% sucrose in 25 mM HEPES (pH = 7.4), prepared according to the method of Stone (Stone, 1974) by overlaying a 5.5 mL solution of 60% sucrose in 25 mM HEPES (pH = 7.4) with 5.5 mL of 20% sucrose in 25 mM HEPES (pH = 7.4) in 12 mL Polyallomer ultracentrifuge tubes (Denville). The tubes were then laid flat for 4 hours at room temperature before being returned to an upright position and placed at 4 °C overnight followed by centrifugation at 218,000G in a SW40Ti rotor for 6 hours. 1 mL fractions were collected from the bottom of the tube and analyzed by Western blotting using affinity purified anti-FtsY at a concentration of 1:2000 and anti-RpoB at 1:10,000 dilution. The membranes were stripped with Restore Western Blot Stripping Buffer (ThermoScientific), rinsed with 1× PBS, and probed with rabbit anti-RecA at a concentration of 1:5,000.

Evolutionary analysis

Orthologous genes of *M. smegmatis* RecA (MSMEG_2723) were obtained through OrthologueDB, which uses a reciprocal BLAST-based algorithm to ensure validity of the orthologous sequences (Whiteside et al., 2013). Briefly, the top BLAST results from an initial search are BLASTed back against the original reference genome, and the results are only counted as orthologs if the top hit in this second search corresponds to the initial sequence of interest. This approach was applied to both *recA* and *ku*. All reciprocal Ortholog results lacking a taxonomy ID (yielding it impossible to identify the species of origin bioinformatically) were disregarded. The *recA* and *ku* databases were subsequently intersected. Organisms that had both *recA* and *ku* coding sequences were considered capable of NHEJ; all others were considered to be capable only of HR. Using taxonomy IDs the KEGG database was then queried for *recA* protein-coding nucleotide sequences.

In order to account for both synonymous and non-synonymous mutations, nucleotide sequences for all organisms were translated into protein sequences, then aligned by Muscle, and finally retranslated back to nucleotide sequences using MEGA6 (Tamura et al., 2013). This multiple alignment was used to test 24 nucleotide substitution models, and the model with the lowest Bayesian information criterion (BIC) score was chosen for computing the pairwise evolutionary distances between each sequence—the general time reversible (GTR) model with a gamma distributed substitution rate (Γ) and an allowance for a proportion of invariant sites (I). The number of base substitutions per site between sequences were used to represent the relative evolutionary distance. Analyses were conducted using the Maximum Composite Likelihood model (Tamura et al., 2004). The rate variation among sites was modeled with a gamma distribution (shape parameter = 1). The analysis involved 1293 nucleotide sequences. All codon positions were included. All ambiguous positions were removed for each sequence pair. There were a total of 6,264 positions in the final dataset. Evolutionary analyses were conducted in MEGA6.

All organisms in the final database were annotated for NHEJ or HR (as mentioned previously), as well as for their amino acid residue corresponding to residue 207 in *M. smegmatis*. Using Matlab, a leaf-optimized *dendrogram* was created using the *linkage*

function from the Statistics Toolbox. For the linkage, 'average' (unweighted average distance) was used as the metric, and the *Euclidean* distance was utilized as the distance metric. The evolutionary distance matrix was converted to a heatmap, and two bars were created to indicate the respective DNA repair pathway the organisms possess, as well as the residue at the relative position of 207.

QUANTIFICATION AND STATISTICAL ANALYSIS

Statistical Analyses

Significance tests were performed in GraphPad Prism. Statistical tests used are reported in the legends of the Main figure legends. All performed statistical tests were two-sided. All error bars represent standard error of the mean (SEM), unless specifically noted otherwise. To assess the difference between percent survival (Fig 2B-E), bacterial growth (Fig 2F), RT PCR gene induction (Fig 3A-D), Rif mutational resistance (Fig 3E-F), and LexA cleavage (Fig 5H), we performed a two-way analysis of variance (ANOVA) test with p values shown in the figure legends. Non-linear regression lines were fit to strand exchange time course data (Fig 4C).

KEY RESOURCES TABLE

REAGENT or RESOURCE	SOURCE	IDENTIFIER
Antibodies		
anti-RecA *(E. coli)*	Abcam	Ab63797
Anti-RecA *(M. smegmatis)*	Pocono Rabbit Farm & Laboratory, Inc.	custom antibodies
anti-RpoB	Biolegend	663905
anti-FtsY	Pocono Rabbit Farm & Laboratory, Inc.	N/A (custom antibody)
Bacterial and Virus Strains		
E. coli BL21 (DE3)	N/A	N/A
Mycobacterium smegmatis MC^{2}155	PMID: 2082148	N/A
Mycobacterium tuberculosis Erdman	N/A	N/A
Biological Samples		
E. coli RecA	New England Biolabs	M0249L
Trypsin-ultra, Mass Spectrometry Grade	NEB	P8101S
Proteinase K	Fisher	FEREO0491
Chemicals, Peptides, and Recombinant Proteins		
1,2-di-(9Z-octadecenoyl)-sn-glycero-d-phosphocoline	Avanti Polar Lipids	850375C
1,2-di-(9Z-octadecenoyl)-sn-glycero-d-phospho-(1′-rac-glycerol)	Avanti Polar Lipids	840475C
1,1′,2,2′-tetra-(9Z-octadecenoyl) cardiolipin	Avanti Polar Lipids	710335C
Kanamycin sulfate from Streptomyces kanamyceticus	Sigma Aldrich	K4000
Hygromycin	Sigma Aldrich	10843555001
L-Lysine dihydrochloride	Sigma Aldrich	L5751
L-Arginine	Sigma Aldrich	A5006

REAGENT or RESOURCE	SOURCE	IDENTIFIER
^{13}C Lysine	Cambridge Isotope Labs	2247-H-0.05
^{13}C Arginine	Cambridge Isotope Labs	U13C6 CLM 2265-H-0.1
Urea	Fisher	U15–500
Tris-HCl	Fisher	BP153–1
Sodium chloride (NaCl)	Fisher	BP358–10
Tris(2-carboxyethyl)phosphine hydrochloride (TCEP)	Sigma	C4706
Iodoacetamide	Sigma	I1149
Acetonitrile (HPLC grade) (ACN)	Fisher	A998–1
Trifluoroacetic acid (TFA)	Sigma	302031
Formic acid	Sigma	F0507
Sodium phosphate dibasic (Na_2HPO_4)	Sigma	255793
Potassium phosphate monobasic (KH_2PO_4)	Sigma	P5655
Phosphate Buffered Saline	Fisher	BP39920
Phosphatase inhibitor 2 and 3	Sigma	P5726 & P0044
cOmplete™ Protease Inhibitor Cocktail	Roche/Sigma	11697498001
dithiothreitol (DTT)	Fisher	R0S61
Ammonium Bicarbonate (NH_4HCO_3)	Fisher	A643
Methyl methanesulfonate	Sigma	129925
isopropyl-β-d-thiogalactoside (IPTG)	Sigma	I675S
Ni-NTA resin	Qiagen	30250
Talon resin	Takara	635502
Titanium dioxide magnetic beads	Pierce	SSS11
ATP, [γ−32P]− 6000Ci/mmol 10mCi/ml Lead, 250 μCi	Perkin Elmer	NEG002Z250UC
Adenosine 5′-[γ-thio]triphosphate tetralithium salt (ATPγS)	Sigma	A13SS-25MG
Piperdine	Sigma	104094
Pyrrolidine	Sigma	P73S03
Tween 80	Sigma	P1754
TLC PEI Cellulose F	Merck Millipore	105579
SDS (Sodium Dodecyl Sulfate)	BioRad	1610302
Dextrose Anhydrous	Fisher	BP350500
Rifampicin	Fisher	BP267925
TRIzol Reagent	ThermoFisher	15596026
Restore Western Blot Stripping Buffer	ThermoFisher	21059
BD Difco Dehydrated Culture Media: Middlebrook 7H9 Broth	Fisher	DF0713–17-9
Remel Middlebrook 7H10 Agar	Fisher	R4539S2
Gibco HEPES	ThermoFisher	15–630-106
Ciprofloxacin	Sigma	17850
Ethylenediaminetetraacetic acid (EDTA)	Sigma	E6758
Lithium Chloride (LiCl)	Sigma	203637

REAGENT or RESOURCE	SOURCE	IDENTIFIER
Streptomycin	Sigma	11860038
Sucrose	Sigma	S0389
Oleic acid	Sigma	01008
Catalase	Sigma	C1345
Anhydrotetracycline Hydrochloride (ATc)	Sigma	94664
M. smegmatis RecA WT	This work	N/A
M. smegmatis RecA S207A	This work	N/A
M. smegmatis RecA S207E	This work	N/A
M. smegmatis RecA S207D	This work	N/A
M. smegmatis RecA S207N	This work	N/A
M. smegmatis LexA	This work	N/A
Critical Commercial Assays		
Thermo Maxima First Strand cDNA synthesis kit	ThermoFisher	K1641
Direct-zol Miniprep Plus kit	Zymo Research	SKU#:R2061
TURBO DNA-free Kit	ThermoFisher	AM1907
BCA assay	Pierce/Thermo Fisher	23250
Oligonucleotides		
/5Alex488N/GA AAA TTC GAC CTA TCC TTG CGC AGC TCG AGA AGC TCT TAC TTT GCG ACC TTT CGC CAT C	IDT	N/A (custom oligo) 488N-ϕX174
GAT GGC GAA AGG TCG CAA AGT AAG AGC TTC TCG AGC TGC GCA AGG ATA GGT CGA ATT TTC	IDT	N/A(custom oligo) ϕX174
TTT TTT TTT TTT TTT TTT TTT TTT TTT TTT	IDT	N/A(custom oligo) oligod
GCACTGGCACATCCTCAC	*M.smegmatis dnaE2* forward primer (this work)	N/A
CCGAACCGGTCCACTAGAT	*M.smegmatis dnaE2* reverse primer (this work)	N/A
ACATGGCCTTTGCGGCATCC	*M.smegmatis dnaE2* TaqMan probe (this work)	N/A
GTCCTGCAATGGGACAAAGA	*M. tuberculosis dnaE2* forward primer (this work)	N/A
CACCAGGTCTTTCGCATAGT	*M. tuberculosis dnaE2* reverse primer (this work)	N/A
CGGCAATCGGCTTGGTGAAATTCG	*M. tuberculosis dnaE2* TaqMan probe (this work)	N/A
Recombinant DNA		
ϕX174 RF1 DNA	NEB	N3021L
Champion™ pET SUMO Expression System	ThermoFisher	K30001
Software and Algorithms		
MEGA6	https://www.megasoftware.net/	N/A
Muscle	https://www.drive5.com/muscle/	N/A
MatLab	https://www.mathworks.com/products/matlab.html	N/A
Custom software (Figure S1)	Github (this paper)	https://github.com/wipper
Xcalibur version: 4.0.27.19	Thermo Fisher Scientific	N/A
GraphPad prism V7	https://www.graphpad.com/scientific-software/prism/	N/A
Image J	https://imagej.nih.gov/ij/	N/A
Other		

REAGENT or RESOURCE	SOURCE	IDENTIFIER
SepPak C18 cartridges	Waters	WAT054945
TSKgel amide-80 column (4.6 mm I.D. x 25 cm packed with 5 μm particles)	Tosoh Biosciences	https://www.separations.e
Extra-Depth disposable petri dish	ThermoFisher	08–757-11Z
Open-Top Polyallomer Ultracentrifuge Tubes, 12.0ml	Denville Scientific	U5030
Nunc OmniTray	Thermo Scientific	140156
SW 40 Ti Swinging-Bucket Rotor	Beckman Coulter	331302
nano ACQUITY UPLC system	Waters	http://www.waters.com/w
Q Exactive plus mass spectrometer	ThermoScientific	http://planetorbitrap.com/
Stratagene UV stratalinker 1800	Stratagene	N/A
Typhoon Trio Variable Mode Imager	GE Healthcare	N/A
Avanti Mini-Extruder	Avanti Polar Lipids	N/A
Zetasizer Nano ZS90	Malvern Panalytical	N/A

CONTACT FOR REAGENT AND RESOURCE SHARING

Further information and requests for resources and reagents should be directed to and will be fulfilled by the Lead Contact, Michael Glickman (glickmam@mskcc.org).

Supplementary Material

Refer to Web version on PubMed Central for supplementary material.

Acknowledgments:

This work was supported by NIH grant AI64693 to MSG, P30 CA008748, and T32 CA009149–40. MFW acknowledges support from the National Center for Advancing Translational Sciences of the National Institutes of Health under Award Number TL1 TR002386–01. The authors wish to thank Yasu Morita for advice about cell fractionation, Nikola Pavletich for advice about the strand exchange assays, and Ken Marians for *E. coli* LexA protein and for critical reading of the manuscript.

References

Adachi J, Hashiguchi K, Nagano M, Sato M, Sato A, Fukamizu K, Ishihama Y, and Tomonaga T (2016). Improved Proteome and Phosphoproteome Analysis on a Cation Exchanger by a Combined Acid and Salt Gradient. Anal. Chem. 88, 7899–7903. [PubMed: 27436111]

Bansal-Mutalik R, and Nikaido H (2014). Mycobacterial outer membrane is a lipid bilayer and the inner membrane is unusually rich in diacyl phosphatidylinositol dimannosides. Proc. Natl. Acad. Sci. 111, 4958–4963. [PubMed: 24639491]

Bell JC, and Kowalczykowski SC (2016). RecA: Regulation and Mechanism of a Molecular Search Engine. Trends Biochem. Sci. xx, 1–17.

Boshoff HI, Reed MB, Barry CE, 3rd, and Mizrahi V (2003). DnaE2 polymerase contributes to in vivo survival and the emergence of drug resistance in Mycobacterium tuberculosis. Cell 113, 183–193. [PubMed: 12705867]

Brooks PC, Movahedzadeh F, and Davis EO (2001). Identification of some DNA damage-inducible genes of Mycobacterium tuberculosis: apparent lack of correlation with LexA binding. J Bacteriol 183, 4459–4467. [PubMed: 11443079]

Chen Z, Yang H, and Pavletich NP (2008). Mechanism of homologous recombination from the RecA-ssDNA/dsDNA structures. Nature 453, 489–4. [PubMed: 18497818]

Cox MM (2007). Regulation of bacterial RecA protein function. Crit Rev Biochem Mol Biol 42, 41–63. [PubMed: 17364684]

Davis EO, Dullaghan EM, and Rand L (2002). Definition of the mycobacterial SOS box and use to identify LexA-regulated genes in Mycobacterium tuberculosis. J. Bacteriol. 184, 3287–3295. [PubMed: 12029045]

Garvey N, St John AC, and Witkin EM (1985). Evidence for RecA protein association with the cell membrane and for changes in the levels of major outer membrane proteins in SOS-induced Escherichia coli cells. J. Bacteriol. 163, 870–876. [PubMed: 3897198]

Gong C, Martins A, Bongiorno P, Glickman M, and Shuman S (2004a). Biochemical and genetic analysis of the four DNA ligases of mycobacteria. J Biol Chem 279, 20594–20606. [PubMed: 14985346]

Gong C, Martins A, Bongiorno P, Glickman M, and Shuman S (2004b). Biochemical and genetic analysis of the four DNA ligases of mycobacteria. J. Biol. Chem. 279, 20594–20606. [PubMed: 14985346]

Gong C, Bongiorno P, Martins A, Stephanou NC, Zhu H, Shuman S, and Glickman MS (2005). Mechanism of nonhomologous end-joining in mycobacteria: a low-fidelity repair system driven by Ku, ligase D and ligase C. Nat. Struct. Mol. Biol. 12, 304–312. [PubMed: 15778718]

Gupta R, Barkan D, Redelman-Sidi G, Shuman S, and Glickman MS (2011). Mycobacteria exploit three genetically distinct DNA double-strand break repair pathways. Mol Microbiol 79, 316–330. [PubMed: 21219454]

Gupta R, Shuman S, and Glickman MS (2015). RecF and RecR play critical roles in the homologous recombination and single-strand annealing pathways of DNA repair in mycobacteria. J. Bacteriol. 197, JB.00290–15.

Hayashi JM, Luo C, Mayfield JA, Hsu T, Fukuda T, and Walfield AL (2016a). Spatially distinct and metabolically active membrane domain in mycobacteria. 113.

Hayashi JM, Luo C-Y, Mayfield JA, Hsu T, Fukuda T, Walfield AL, Giffen SR, Leszyk JD, Baer CE, Bennion OT, et al. (2016b). Spatially distinct and metabolically active membrane domain in mycobacteria. Proc. Natl. Acad. Sci. U. S. A. 113, 5400–5405. [PubMed: 27114527]

Kettenbach AN, and Gerber SA (2011). Rapid and Reproducible Single-Stage Phosphopeptide Enrichment of Complex Peptide Mixtures: Application to General and Phosphotyrosine-Specific Phosphoproteomics Experiments. Anal. Chem. 83, 7635–7644. [PubMed: 21899308]

Lesterlin C, Ball G, Schermelleh L, and Sherratt DJ (2013). RecA bundles mediate homology pairing between distant sisters during DNA break repair. Nature 506, 249–253. [PubMed: 24362571]

Morita YS, Sena CB, Waller RF, Kurokawa K, Sernee MF, Nakatani F, Haites RE, Billman-Jacobe H, McConville MJ, Maeda Y, et al. (2006). PimE is a polyprenol-phosphate-mannose-dependent mannosyltransferase that transfers the fifth mannose of phosphatidylinositol mannoside in mycobacteria. J Biol Chem 281, 25143–25155. [PubMed: 16803893]

Movahedzadeh F, Colston MJ, and Davis EO (1997). Characterization of Mycobacterium tuberculosis LexA: recognition of a Cheo (Bacillus-type SOS) box. Microbiology 143 (Pt 3, 929–936. [PubMed: 9084177]

Nautiyal A, Patil KN, and Muniyappa K (2014). Suramin is a potent and selective inhibitor of Mycobacterium tuberculosis RecA protein and the SOS response: RecA as a potential target for antibacterial drug discovery. J. Antimicrob. Chemother. 69, 1834–1843. [PubMed: 24722837]

Polo SE, and Jackson SP (2011). Dynamics of DNA damage response proteins at DNA breaks: a focus on protein modifications. Genes Dev 25, 409–433. [PubMed: 21363960]

Prisic S, Dankwa S, Schwartz D, Chou MF, Locasale JW, Kang CM, Bemis G, Church GM, Steen H, and Husson RN (2010). Extensive phosphorylation with overlapping specificity by Mycobacterium tuberculosis serine/threonine protein kinases. Proc Natl Acad Sci U S A 107, 7521–7526. [PubMed: 20368441]

Rajendram M, Zhang L, Reynolds BJ, Auer GK, Tuson HH, Ngo KV, Cox MM, Yethiraj A, Cui Q, and Weibel DB (2015). Anionic Phospholipids Stabilize RecA Filament Bundles in Escherichia coli. Mol. Cell 60, 374–384. [PubMed: 26481664]

Sherman DR, and Grundner C (2014). Agents of change - concepts in Mycobacterium tuberculosis Ser/Thr/Tyr phosphosignalling. Mol. Microbiol. 94, 231–241. [PubMed: 25099260]

Smollett KL, Smith KM, Kahramanoglou C, Arnvig KB, Buxton RS, and Davis EO (2012a). Global analysis of the regulon of the transcriptional repressor LexA, a key component of SOS response in Mycobacterium tuberculosis. J Biol Chem 287, 22004–22014. [PubMed: 22528497]

Smollett KL, Smith KM, Kahramanoglou C, Arnvig KB, Buxton RS, and Davis EO (2012b). Global Analysis of the Regulon of the Transcriptional Repressor LexA, a Key Component of SOS Response in Mycobacterium tuberculosis. J. Biol. Chem. 287, 22004–22014. [PubMed: 22528497]

Stone AB (1974). A simplified method for preparing sucrose gradients. Biochem. J. 137, 117–118. [PubMed: 4595281]

Tamura K, Nei M, and Kumar S (2004). Prospects for inferring very large phylogenies by using the neighbor-joining method. Proc. Natl. Acad. Sci. U. S. A. 101, 11030–11035. [PubMed: 15258291]

Tamura K, Stecher G, Peterson D, Filipski A, and Kumar S (2013). MEGA6: Molecular Evolutionary Genetics Analysis version 6.0. Mol. Biol. Evol. 30, 2725–2729. [PubMed: 24132122]

Warner DF, Ndwandwe DE, Abrahams GL, Kana BD, Machowski EE, Venclovas C, and Mizrahi V (2010a). Essential roles for imuA'- and imuB-encoded accessory factors in DnaE2-dependent mutagenesis in Mycobacterium tuberculosis. Proc. Natl. Acad. Sci. U. S. A. 107, 13093–13098. [PubMed: 20615954]

Warner DF, Ndwandwe DE, Abrahams GL, Kana BD, Machowski EE, Venclovas C, and Mizrahi V (2010b). Essential roles for imuA'- and imuB-encoded accessory factors in DnaE2-dependent mutagenesis in Mycobacterium tuberculosis. Proc. Natl. Acad. Sci. U. S. A. 107, 13093–13098. [PubMed: 20615954]

Whiteside MD, Winsor GL, Laird MR, and Brinkman FSL (2013). OrthologeDB: a bacterial and archaeal orthology resource for improved comparative genomic analysis. Nucleic Acids Res. 41, D366–76. [PubMed: 23203876]

Zhang L, Rajendram M, Weibel DB, Yethiraj A, and Cui Q (2016). Ionic Hydrogen Bonds and Lipid Packing Defects Determine the Binding Orientation and Insertion Depth of RecA on Multicomponent Lipid Bilayers. J. Phys. Chem. B 120, 8424–8437. [PubMed: 27095675]

Highlights:

- Mycobacterial RecA is phosphorylated at Serine 207 after DNA damage
- RecA phosphorylation inhibits RecA coprotease activity and SOS-dependent mutagenesis
- RecA associates with the membrane post DNA damage
- Serine 207 also controls cardiolipin-based inhibition of the RecA coprotease

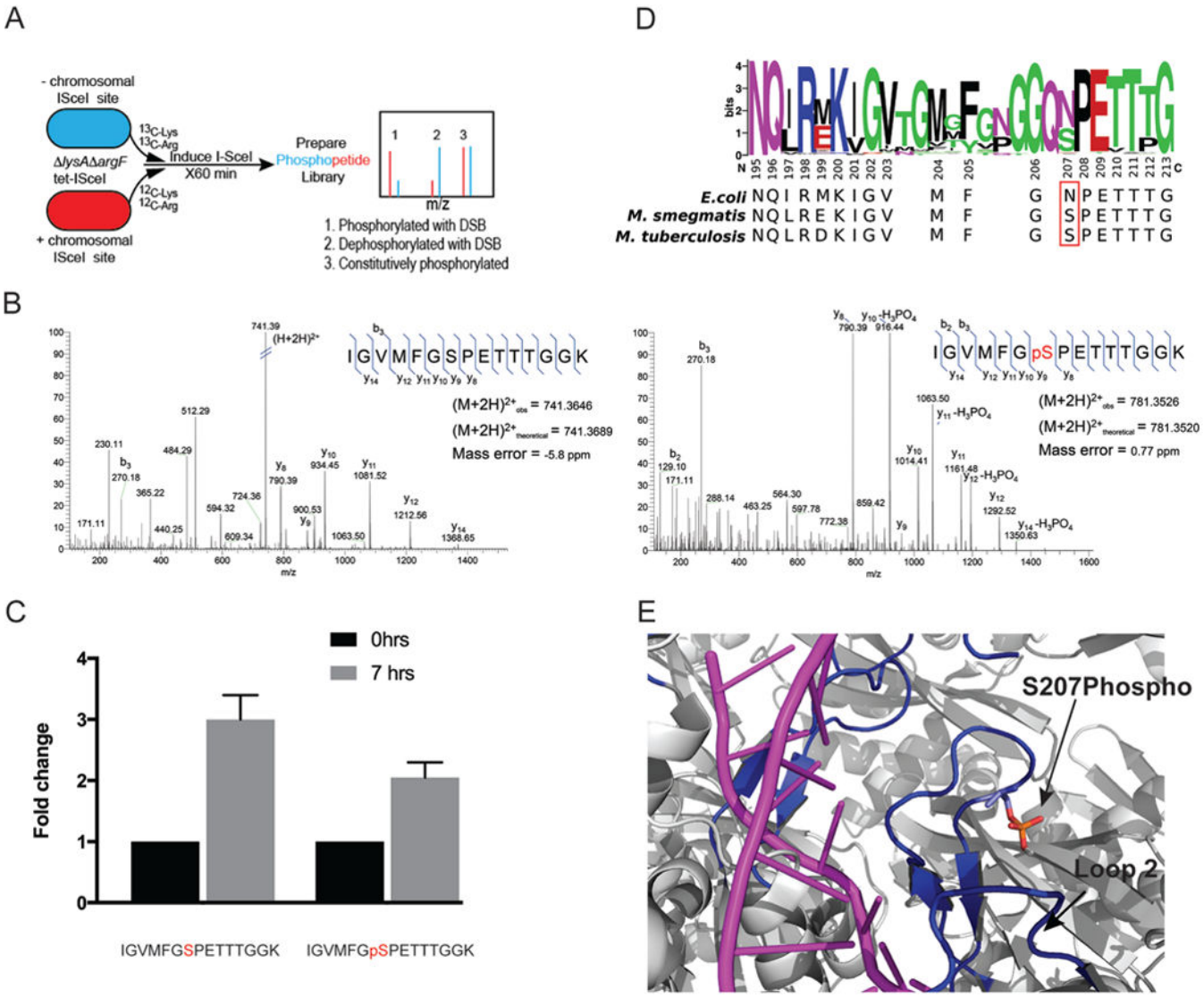

Figure 1- RecA is phosphorylated on serine S207 during the DNA damage response

(A) Schematic of the SILAC screen. Two strains of Δ*lysA*Δ*argF* tet-I-SceI *M. smegmatis* were compared, one carrying a chromosomal cleavage site for I-SceI and one without a cleavage site. Labeling with ^{13}C lysine and ^{13}C arginine was followed by one hour of I-SceI induction. Phosphopeptide libraries were prepared and analyzed by quantitative mass spectroscopy. Three patterns of phosphorylation are depicted: 1) phosphorylation induced by DSB 2) dephosphorylation with DSB and 3) constitutively phosphorylated. (B) MS/MS detection of the S207-phosphopeptide. The left panel shows the non-phosphorylated RecA-L2 peptide and the right panel shows the RecA-L2-S207 phosphopeptide. In both cases, the observed and predicted mass ions are shown. The fragment ions of each peptide are indicated on the peptide sequence with corresponding peaks labeled on the chromatogram. (C) RecA S207 phosphopeptide accumulates after DNA damage. Wild type *M. smegmatis* bearing a tetracycline inducible cas9 and a guide RNA targeting the nonessential *dnaJ2* gene was induced with anhydrotetracycline for 7 hours. The relative increase in RecA 201–215 and RecA 201–215 phosphopeptide is shown, with uninduced cells set to 1 for each peptide.

(D) RecA Loop 2 is highly conserved. The amino acids of RecA loop 2 derived from 1,293 RecA sequences from Bacteria and Archaea were aligned and used to generate the alignment with the mycobacterial RecA numbering below the logo. The amino acid sequences of *E. coli*, *M. smegmatis,* and *M. tuberculosis* L2 are shown with the phosphorylated S207 (N in *E. coli)* boxed in red.(E) RecA L2 becomes ordered in the presynaptic nucleoprotein filament. PDB structure 3CMX of the *E. coli* RecA presynaptic filament was modified to substitute phospho serine at N206 (Chen et al., 2008). RecA L2 from two adjacent RecA monomers is colored blue, dsDNA in purple, and the background RecA structure in grey.

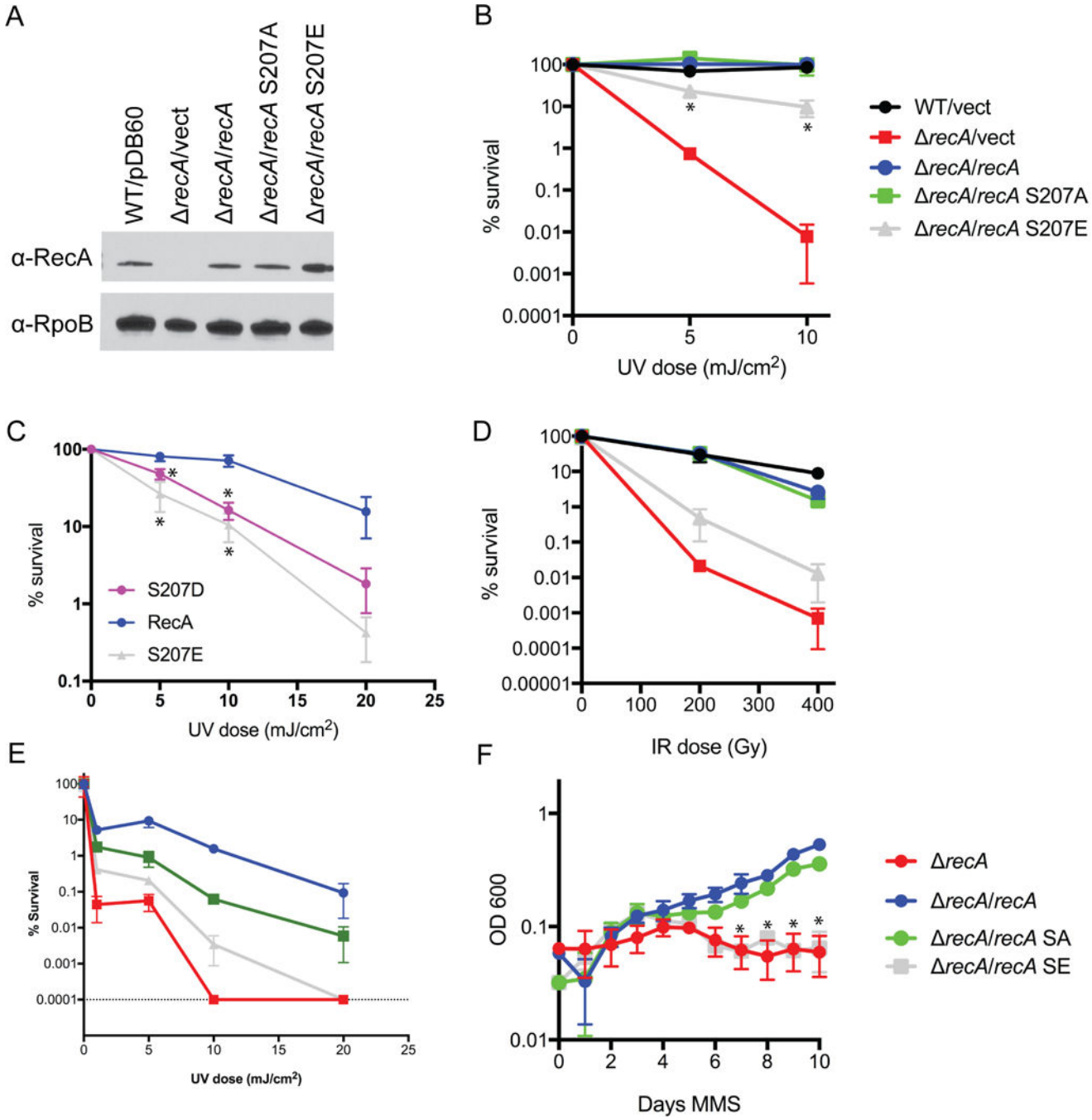

Figure 2- Loop 2 phosphorylation suppresses the DNA damage response

(A) α-RecA western blot of mid-log phase expression of RecA protein in the following *M. smegmatis* strains: WT+Vector (pDB60), Δ*recA*+vector, Δ*recA+recA*, Δ*recA+recA* S207A, S207E. α-RpoB is used as a loading control. B,C Phosphomimetic substitutions at S207 inhibit DNA repair. *M. smegmatis* strains of the indicated genotype were treated with the indicated doses of UV light and survival was determined by culturing serial dilutions on agar media. % survival is plotted on the logarithmic Y axis. Vect = vector control. *=p<0.01 by ANOVA for comparison to WT. n=3 biological replicates *D. M. smegmatis* strains of the

indicated genotype were treated with 200/400 Gy of ionizing radiation and survival was determined by culturing serial dilutions on agar media. % survival is plotted on the logarithmic Y axis. Strain key is the same as in panel B. *=$p<0.01$ by ANOVA. n=3 biological replicates E. *M. tuberculosis* strains were treated with the indicated does of UV light and survival plotted as in (B). n=3 biological replicates F *M. tuberculosis* strains of the indicated genotype were treated with 0.2% MMS as described in materials and methods and bacterial growth was quantitated by measuring OD_{600} over time. *=$p<0.01$ by ANOVA. n=3 biological replicates

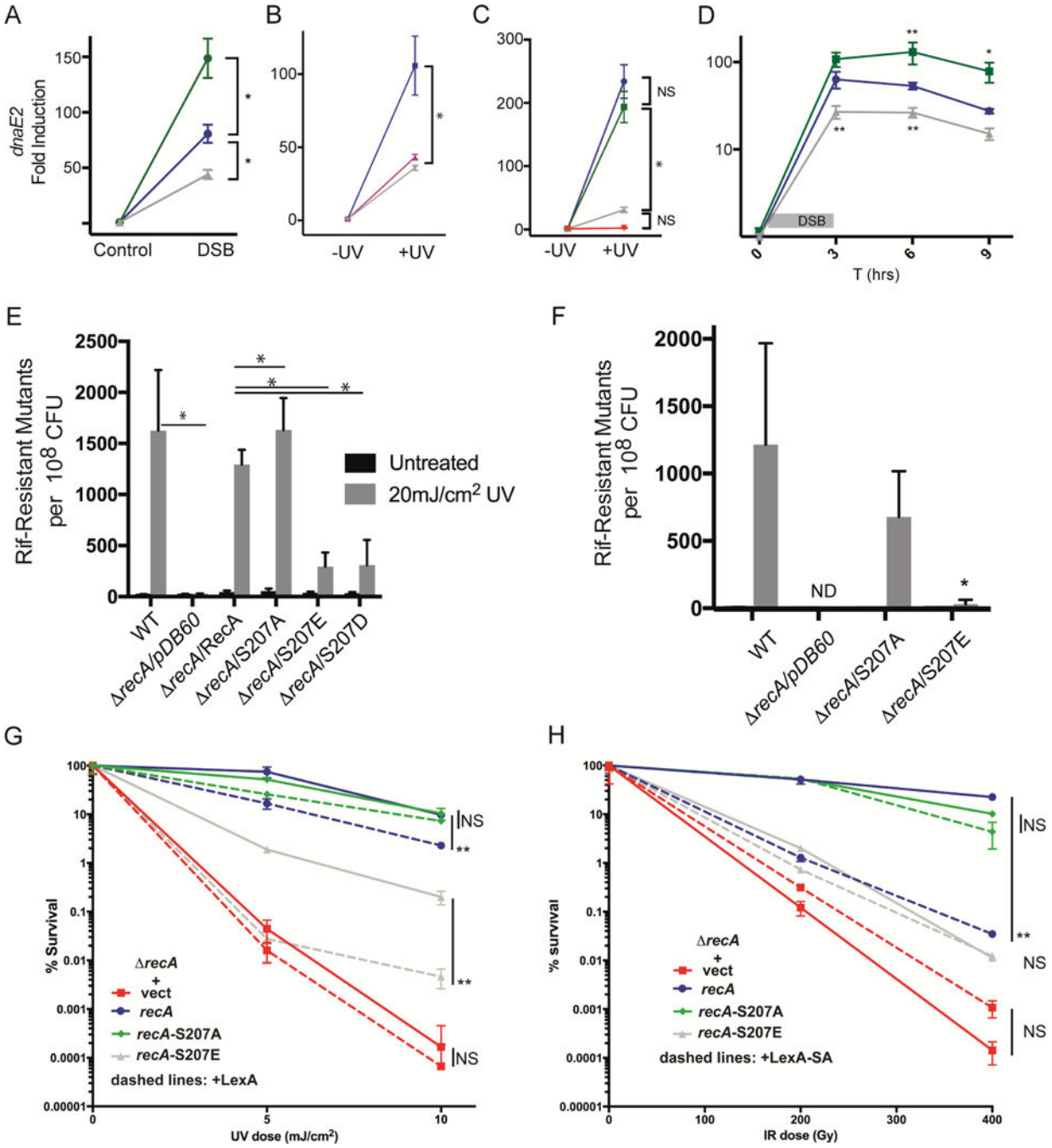

Figure 3. RecA S207 phosphorylation controls RecA coprotease function in vivo

(A,B,C) RecA S207 phosphorylation suppresses transcriptional induction of *dnaE2,* an SOS target. Shown are normalized mRNA levels for the RNA encoding *dnaE2* in *M. smegmatis* treated with quinolones to induce DSBs (A) UV (B) or *M. tuberculosis* treated with UV (C). Strains are: Δ*recA+recA* (blue), Δ*recA+recAS207A* (green), Δ*recA+recAS207E* (grey), Δ*recA+recAS207D* (magenta,(B)) or Δ*recA*+vector (red). The Y axis is *dnaE2* mRNA fold induction over time 0 (set to 1), error bars are SEM and * indicates $p < 0.01$ by ANOVA. n=3 biological replicates for all experiments (D) S207 phosphorylation affects the kinetics of

SOS resolution. Color scheme is the same as panel A. *M. smegmatis* of the indicated genotype were exposed for ciprofloxacin for 3 hours (grey box) followed by washing to remove the clastogen and *dnaE2* RNA was quantitated over time. **=p<0.01, *=p<0.05, both by t test of the indicated mutant vs wild type. n=2 biological replicates (E,F) RecA S207 phosphorylation suppresses chromosomal mutagenesis in *M. smegmatis* and *M. tuberculosis*. Frequency of rifampin resistant mutants per 10^8 cells in untreated (black bars) or UV treated (grey bars) *M. smegmatis* (E) *or M. tuberculosis* (F) cells of the indicated genotype expressing RecA proteins with phosphomimetic or ablative substitution at S207. Bars and * indicate $p < 0.001$ for the indicated comparisons by ANOVA. ND=not detected. n=10 biological replicates except for S207A (n=9) and S207D (n=5). (G) RecAS207 phosphorylation suppresses SOS through impaired LexA co-protease function. *M. smegmatis* Δ*recA* was complemented either with vector (red) or RecA alleles encoding substitutions at S207 (blue, wild type RecA; green S207A; grey S207E) with (dashed lines) or without (solid lines) coexpression of the LexA repressor. Statistical significance indicated by ** ($p < 0.01$) for comparison of each +/− LexA pair. n = 3 biological replicates. Error bars represent SEM. (H) The DNA damage sensitivity imparted by RecA phosphorylation is epistatic with a LexA uncleavable allele. The color scheme is identical to panel A, with the dashed lines indicating LexA S167A (LexA-SA), which cannot undergo RecA stimulated autoproteolysis. Statistical significance indicated by ** ($p < 0.01$) for comparison of each +/− LexA-S167A pair. n = 3 biological replicates. Error bars represent SD.

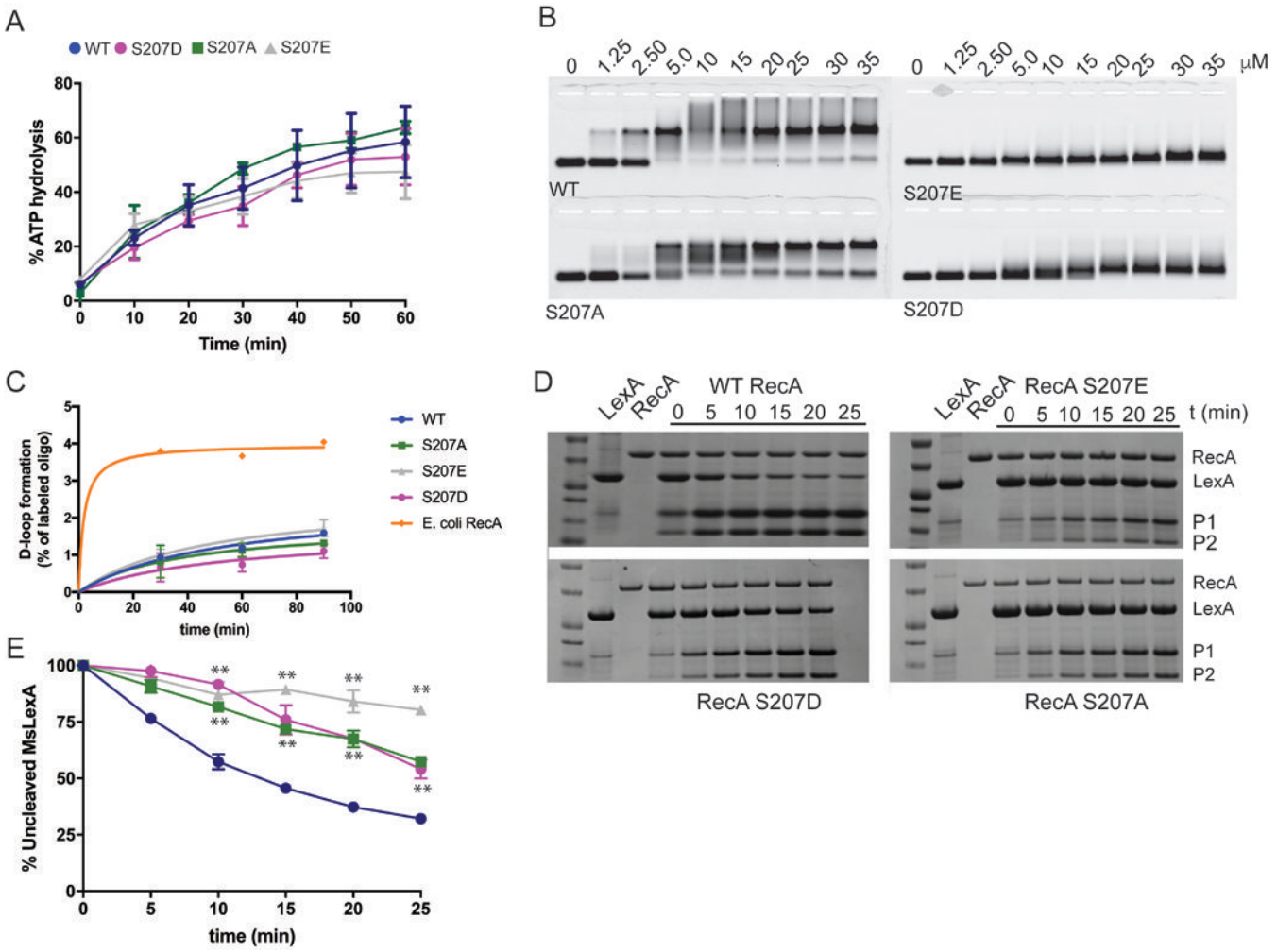

Figure 4: RecA S207 phosphomimetic specifically impairs LexA coprotease activity.

(A) Progress curves of ATP hydrolysis of the indicated RecA proteins. Each point is the mean of 2 replicates and error bars are SD. (B) Electrophoretic mobility shift (EMSA) assay of 60-mer ϕX174-oligo incubated with increasing concentrations of the indicated RecA proteins (from 0–35μM). Shown is a single EMSA technical replicate. (C) Strand exchange activity of S207 substituted RecA proteins compared to *E. coli* RecA. See Figure S3 and methods for full characterization of the D loop assay. Quantitation was performed on two technical replicates. (D) Phosphomimetic substitution at RecA S207 impairs LexA cleavage by the RecA nucleoprotein filament. Each panel is a Coomassie stained SDS PAGE gel of a LexA cleavage reaction containing 10 μM LexA protein, RecA nucleoprotein filaments (3 μM RecA and 10 μM 60 mer ssDNA). RecA, LexA and two LexA cleavage products (P1 and P2) are labeled. The first two lanes after the MW marker are LexA and RecA alone, followed by a time course from 0 – 25 minutes. (E) Quantitation of the LexA cleavage in duplicate experiments over time by the indicated RecA proteins. ** indicates $p<0.0001$ for each protein vs WT RecA at the indicated time points. Color scheme is the same as panel A.

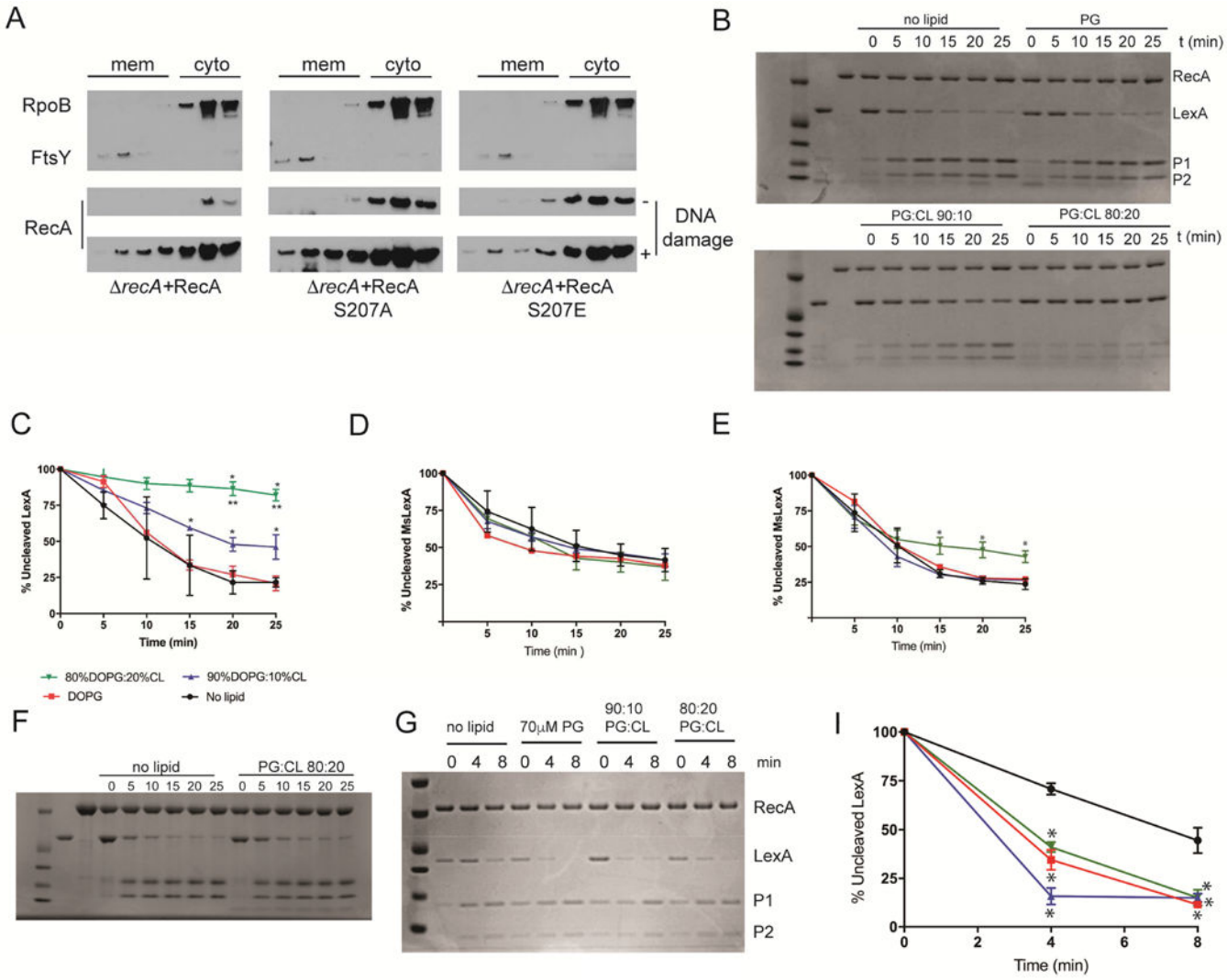

Figure 5. Membrane phospholipids control RecA coprotease function through S207

(A) RecA associates with the membrane during the DDR independent of phosphorylation. *M. smegmatis* cells of the indicated genotype unexposed or exposed to ciprofloxacin (+/− DNA damage) were lysed and fractionated on a sucrose gradient as described in materials and methods. Membrane and cytoplasmic fraction assignments based on western blotting with antibodies to the marker proteins RpoB (cytoplasmic) and FtsY (membrane) shown in the top panel. Anti-RecA antibodies were used to probe the lower two panels. Shown is a representative of three biological replicates (B) Cardiolipin inhibits the WT RecA coprotease activity for LexA. LexA cleavage reactions containing RecA nucleoprotein filaments and LexA were performed with no vesicles (no lipid), anionic vesicles containing phosphatidylglycerol (PG), anionic vesicles containing 90:10 PG: Cardiolipin (CL), or 80:20 PG:CL. (C-E) Quantitation of LexA cleavage. WT RecA (C), RecA S207E (D), RecA S207A (E) with no lipid (black), PG vesicles (red), 90:10 PG:CL vesicles (blue), or 80:20 PG:CL (green). * indicates $p < 0.01$ for each vesicle in comparison to no lipid. ** indicates $p < 0.01$ for the comparison of 80:20 vs 90:10. Quantitation was performed on three

technical replicates. (F) Substitution of the *E. coli* asparagine at S207 confers resistance to cardiolipin inhibition. LexA cleavage reactions as in panel B with RecAS207N protein and either no lipid, or 80:20 PG:CL vesicles. (G,H). Phospholipids enhance the LexA coprotease activity of *E. coli* RecA. G. 8 minute LexA cleavage reactions containing either no lipid, 70μM phosphatidylglycerol vesicles, and either 90:10 or 80:20 PG:Cardiolipin. H. Quantitation of *E. coli* LexA cleavage. *=p<.001 using 2 way ANOVA compared to no lipid. Color scheme is the same as C-E. Quantitation was performed on two technical replicates.

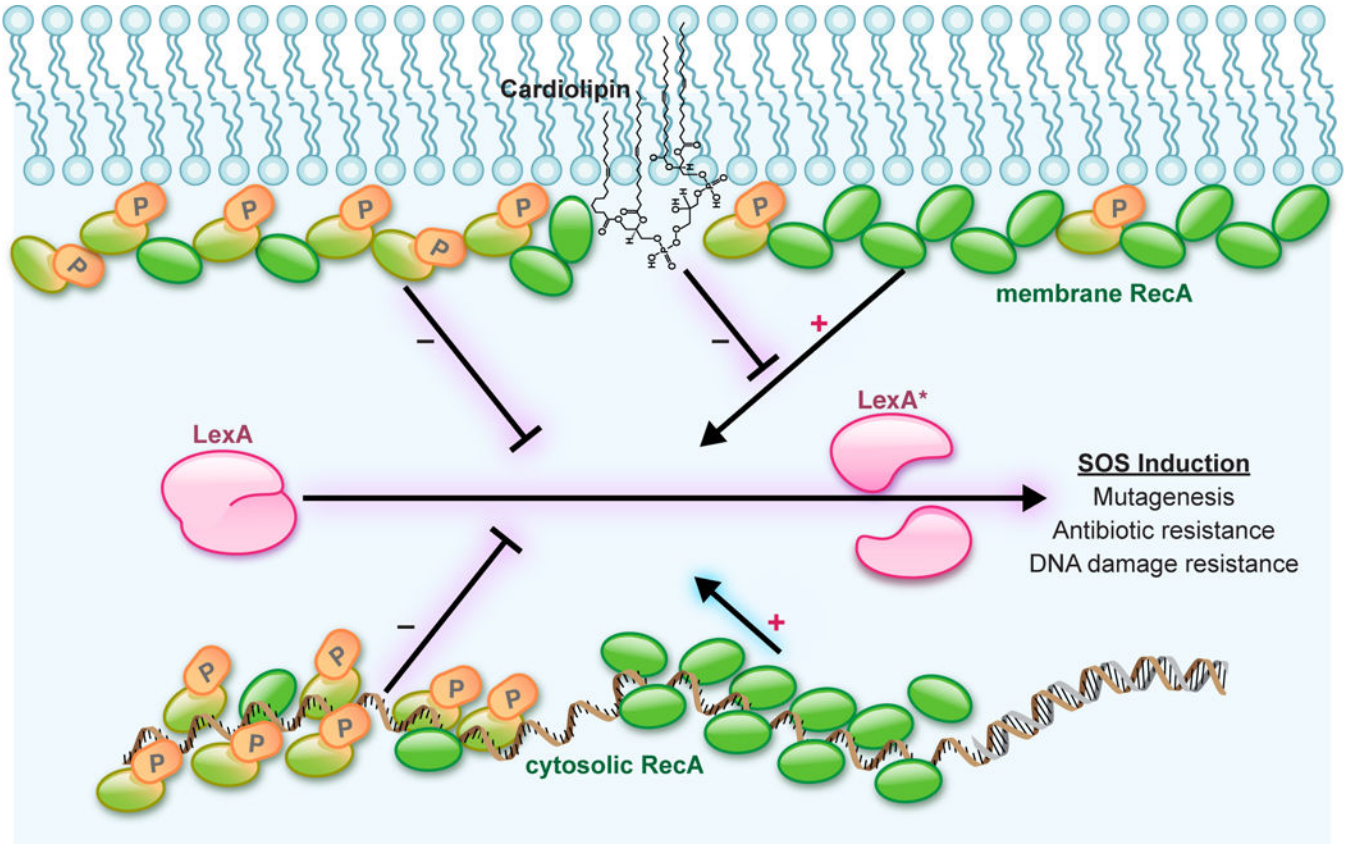

Figure 6: Model for dual control of RecA catalyzed LexA cleavage through phosphorylation and cardiolipin converging on L2 S207.

With the induction of DNA damage and formation of RecA nucleoprotein filaments, these filaments serve as the coprotease for the autoproteolysis of LexA and induction of the SOS response, with consequent mutagenesis and antibiotic resistance. There are two pools of RecA during the DNA damage response, cytoplasmic and membrane associated. Within these two pools, RecA can either be phosphorylated on serine 207 or unphosphorylated. Phosphorylation of RecA on Serine 207 inhibits this coprotease activity. In addition, membrane cardiolipin can inhibit this coprotease activity of wild type RecA, but not RecA carrying an S207 phosphorylation, indicating that both mechanisms (phosphorylation and cardiolipin) converge on the Loop 2 S207 residue to control the DNA damage response in mycobacteria.